AD_____

Award Number: W81XWH-14-1-0288

TITLE:
High-Resolution Radioluminescence Microscopy for the Study of Prostate Tissue Slice Cell Metabolism and Monitoring of Treatment Response

PRINCIPAL INVESTIGATOR: Silvan Tuerkcan, PhD

CONTRACTING ORGANIZATION:
Leland Stanford Junior University, The
Stanford CA 94305-2004

REPORT DATE: October 2015

TYPE OF REPORT: annual

PREPARED FOR: U.S. Army Medical Research and Materiel Command
Fort Detrick, Maryland 21702-5012

DISTRIBUTION STATEMENT:

X Approved for public release; distribution unlimited

REPORT DOCUMENTATION PAGE

Form Approved
OMB No. 0704-0188

1. REPORT DATE *(DD-MM-YYYY)*	**2. REPORT TYPE**	**3. DATES COVERED** *(From - To)*
October 2015	Annual Report	30 Sep 2014 - 29 Sep 2015

4. TITLE AND SUBTITLE
High-Resolution Radioluminescence Microscopy for the Study of Prostate Tissue Slice Cell Metabolism and Monitoring of Treatment Response

5a. CONTRACT NUMBER

5b. GRANT NUMBER
W81XWH-14-1-0288

5c. PROGRAM ELEMENT NUMBER

6. AUTHOR(S)
Silvan Tuerkcan (PI)

5d. PROJECT NUMBER

5e. TASK NUMBER

5f. WORK UNIT NUMBER

7. PERFORMING ORGANIZATION NAME(S) AND ADDRESS(ES)
Stanford University School of Medicine
Department of Radiation
Oncology
1050 A Arastradero
Palo Alto, 94304 CA

8. PERFORMING ORGANIZATION REPORT NUMBER

9. SPONSORING / MONITORING AGENCY NAME(S) AND ADDRESS(ES)
U.S. Army Medical Research and
Materiel Command
Fort Detrick, Maryland
21702-5012

10. SPONSOR/MONITOR'S ACRONYM(S)
DoD

11. SPONSOR/MONITOR'S REPORT NUMBER(S)

12. DISTRIBUTION / AVAILABILITY STATEMENT

Approved for public release; distribution is unlimited

13. SUPPLEMENTARY NOTES

14. ABSTRACT

Currently, prostate cancers are classified using the Gleason Grade system and immunohistochemistry. The shortcoming of this method is that it requires fixation, which kills the cells in the tissue sample. We want to develop an optical microscopy method that can provide a high resolution (a few cells) image of the local metabolism in prostate cancer tissue slice cultures (TSCs). Our ***hypothesis*** is that the local glucose concentration in prostate TSCs is correlated to the malignancy of the disease. We aim at developing a microscopy technology to image the uptake of radiotracers into prostate TSCs with a high resolution. This will yield additional information on the metabolic activity of the tissue, which may be used to improve staging of a biopsy or to study the uptake of new tracers in vivo.

15. SUBJECT TERMS

16. SECURITY CLASSIFICATION OF:			**17. LIMITATION OF ABSTRACT**	**18. NUMBER OF PAGES**	**19a. NAME OF RESPONSIBLE PERSON** USAMRMC
a. REPORT	**b. ABSTRACT**	**c. THIS PAGE**		11	**19b. TELEPHONE NUMBER** *(include area code)*

Standard Form 298 (Rev. 8-98)
Prescribed by ANSI Std. Z39.18

Contents

Introduction

Prostate cancer is the second most common cancer occurring among American men, with 241,740 men diagnosed in the United States in 2012. Increased screening, such as using serum prostate-specific antigen (PSA) and extended-template transrectal ultrasound biopsies, have led to the earlier detection and staging of patients, but clinical management of the disease remains difficult. This difficulty is primarily due to the biological diversity in prostate cancers, which often arise from multiple sites in the prostate. A major challenge in the field of prostate cancer is to correctly identify if a cancer is aggressive and dangerous for the patient and if the cancer will or will not impact the patient's quality of life. Currently, prostate cancers are classified from biopsies after immunohistochemistry using a modified version of the Gleason Grading System. It is also important to monitor the aggressiveness of cancer cells during biological experiments in tissue slices for example to study the efficacy of a new treatment in vitro. It is thus imperative to develop a new microscopy method that can provide a measure of cell activity.

The purpose of the work is to provide an optical tool to measure the local metabolism in live tissue slices for biological studies of treatment efficacies. We aim at developing an optical microscopy method that can provide supplemental information based on the local metabolism of cells within the tissue.

Our main hypothesis is that the locally resolved metabolism of cells is a robust indicator of the malignancy of the cancer. The Warburg effect predicts that the metabolism of cancer cells differs from the metabolism of the other cells in the prostate tissue in such a way that cancer cells use more glucose than normal cells [1,2]. This effect is exploited in positron emission tomography (PET) imaging, where cancer cells are imaged due to their higher metabolic rate of radiolabeled glucose, such as fluorodeoxyglucose (FDG). Clinically, this hypothesis could have broad implications for studying the efficacy of treatments. However, a current limitation is that the uptake of FDG cannot be resolved within individual cells using conventional instrumentation such as PET, autoradiography, and scintillation counting. However, the technology that will be developed over the course of this project will be able to provide the required resolution.

The rationale for our hypothesis is: tumor cells take up more glucose when compared to normal tissue. This effect has been used to enable PET imaging and significantly increased glucose metabolism in cancers correlates well with higher histologic grades and poor survival [3,4].

Keywords

Prostate cancer tissue culture, radioluminescence microscopy, radiotracer, FDG, metabolism, image analysis, disease staging.

Timeline

This reports is the first annual report of the two year project (months 1-12). For a better understanding of the progress, we reproduce the work statement summary at this point. We have colored all achieved objectives and tasks in green.

Task	Month 1-6	Month 7-12	Month 13-18	Month 19-24
Objective 1: Design of a radioluminescence microscope for the imaging of FDG uptake in Prostate tissue slice cultures (TSCs).				
Task 1: Set-up				
Task 2: Algorithm				
Task 3: FDG calibration				
Task 4: FDG imaging in TSCs				
Objective 2: Comparative measurements of FDG uptake into prostate TSCs of Gleason Grade 3 and 4/5 in vitro.				
Task 7: Correlation algorithm				
Task 8: In vitro FDG imaging in TSCs				
Task 9: Statistical data analysis				
Objective 3: Proof-of-concept measurements of the cell metabolism in live TSCs during radiation treatment.				
Task 12: FDG imaging with irradiation				

Key Research Accomplishments

Objective 1: Design of a radioluminescence microscope for the imaging of FDG uptake in prostate tissue slice cultures (TSCs).

Task 1:

We successfully built an inverted fluorescence microscopy platform to image the FDG distribution in TSCs. To image the FDG content on a single-cell level, we turn to RLM, which is presented in Ref. [5] (Fig. 1). The advantage of the technique is that decays are converted to an optical signal close to the origin of the decay, which enables decay detection with single-cell resolution. Live cells are sparsely cultured on a glass coverslip and are incubated with FDG. RLM utilizes a thin scintillator plate, which is in contact with the cells of interest, to convert ionizing radiation from emitted beta particles into visible-range photons detectable in a sensitive microscope. The optical scintillation signal can be measured with an EM-CCD camera with high resolution and enables minute radiotracer detection. An optimized set-up produces the while light cell image and the corresponding RLM image in Fig 1 B (Task 1b).

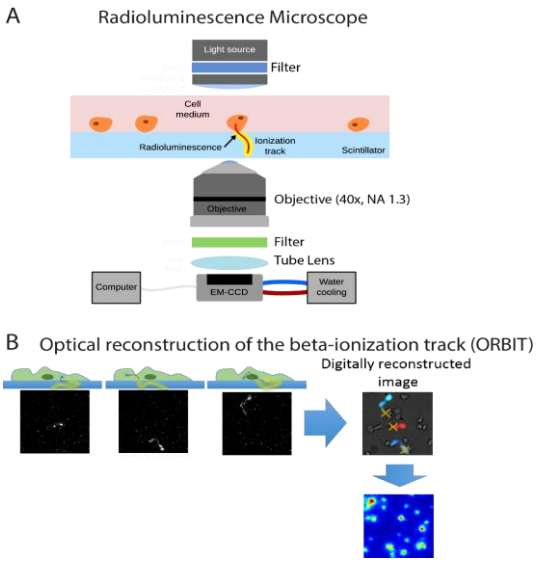

Figure 1. Schematics of the radioluminescence microscope and image reconstruction. (A) A decay event of the 18 F atom in the FDG will generate a β-particle, which will travel up to 100 µm in water. The scintillator will generate visible photons along the trajectory of a β-particle, which are collected by a high NA microscope (Olympus LV200). (B) The radioluminescence image was obtained by our methodology called "optical reconstruction of the beta-ionization track" (ORBIT) as described in detail in Pratx *et al.* [6] and in the methods section. Individual decays are imaged with a high acquisition time and their center of mass is recorded to build up a 2D histogram of decays, which is the digitally reconstructed FDG image.

We also compared the performance of new thin-film scintillators (Lu_2O_3) to the performance of the thicker standard $CdWO_4$ scintillators (Task 1c). The data is shown in the following table and figure 2:

Scintillator type	Light yield [photons keV^{-1}]	Emission maximum [nm]	Effective Z (atomic number)	Total stopping power[a] [MeV cm^{-1}]	Hygroscopic	Thickness [µm]	Density [g cm^{-3}]
Lu_2O_3:Eu	48	610	67.3	21.4	No	6–10	9.5
$CdWO_4$ 12–15	480	64	19.0	No	500	7.9	

[a]Stopping power given for 100 keV positron.

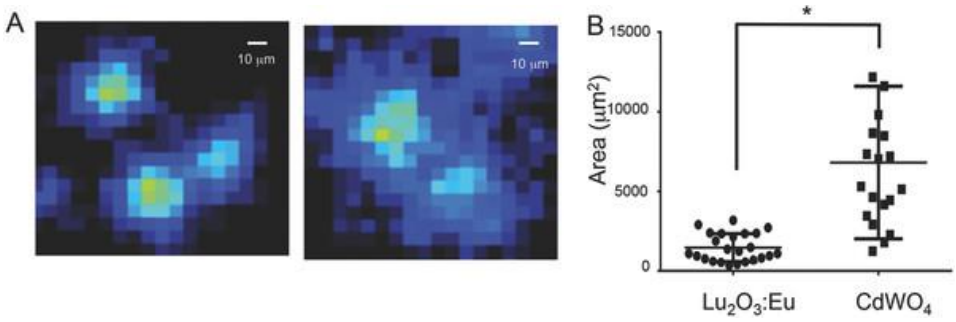

Figure 2. Performance of thin film scintillators. (A) Shows a side by side comparison of the thin-film scintillators (Lu_2O_3, left) and the standard $CdWO_4$ scintillators (right). Analysis shows a smaller area of the tracks within the thin film scintillator, which leads to a higher resolution.

Thin film scintillators provide better image resolution, but the manufacturing of this material is difficult. That is why we will continue using commercial $CdWO_4$ scintillators for the remainder of this work.

Task 2:

We implemented a digital reconstruction algorithm to reconstruct individual decays within the sample into a final distribution or image. The method filters and thresholds individual images to detect decay events using a center-of-mass location step. The reconstruction is shown in figure 1 B. The parameters of the thresholding are adjusted every time a new sample is analyzed. The false detection rate is below 0.1%.

Task 3:

We calibrated the microscope using a thin film of FDG in matrigel. The advantage of this method is that we know the exact thickness of the film and thus the imaged volume and activity in the field of view. With

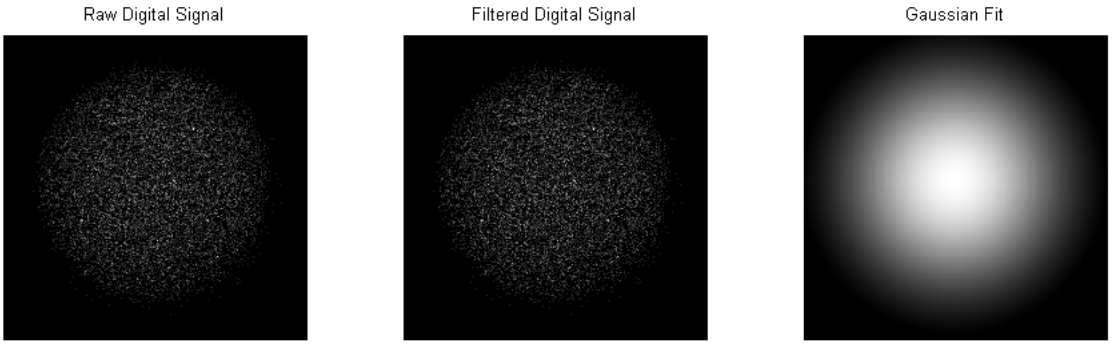

Figure 3. Image from a homogeneous distribution of radiotracers, with the corresponding Gaussian fit to correct for the position of an emitting object in the field of view.

the decay rate and the profile of the collected data we calibrated the microscope to be able to report measurements in Becquerel (Bq) and we also correct for the collection deficiencies towards the border of the image by fitting the pattern of decays, as shown in figure 3. Drift did not manifest itself as a problem during experiments.

Task 4:

With the RLM microscope we set out to optimize the protocol for tissue imaging. The optimized protocol is as follows:

1. Starvation of the prostate TSCs in glucose-free media for 45 minutes.
2. Incubation of prostate TSCs in glucose-free media with 100 µCi/mL ^{18}F-FDG for 10 minutes.
3. Subsequent rinsing steps to remove excess FDG.
4. Fixation in 4% paraformaldehyde for 10 minutes.
5. Cherenkov imaging to localize tumors and regions of interest.
6. Cryosectioning into 8 µm slices and transfer onto imaging coverslip.
7. RLM microscopy
8. H&E staining of the same section.
9. Image analysis

The protocol and workflow is shown in Fig. 4.

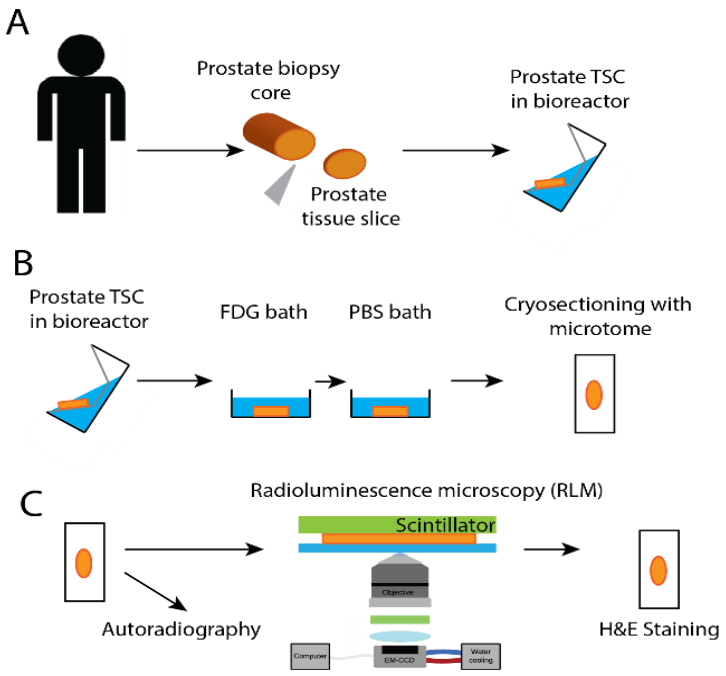

Figure 4: (A) Prostate biopsies are taken following radical prostatectomy. The biopsy cores are sectioned into 200 µm sections, which are kept alive in a bioreactor and serve as a faithful tissue culture model [1]. (B) Prior to imaging, tissue slice cultures (TSCs) are starved in low glucose media and incubated in media containing 100 µCi/mL FDG. After rinsing with PBS, the TSCs are sectioned into 8 µm slices using a microtome and transferred onto a glass coverslip. (C) These slices are then imaged by autoradiography or radioluminescence microscopy (RLM), which gives a high resolution image of the FDG distribution. Slices are then H&E stained for histology.

This protocol was first developed with human clear cell renal carcinoma samples due to the abundance of these samples.

Objective 2: Comparative measurements of FDG uptake into prostate TSCs of Gleason Grade 3 and 4/5 in vitro.

Task 7:

We have determined that the development of an image correlation algorithm to overlap radioluminescence measurements and immunohistochemistry (task 7) results is not necessary. It is in fact possible to stain the exact TSC slice we image in RLM following the experiment. The quality of the H&E slices are good enough to perform a direct comparison, which removes the need for the correlation algorithm. However, we have decided to replace the correlation algorithm with a machine vision algorithm that can automatically detect suspicious features in a sample. We will implement this algorithm in our analysis of task 9.

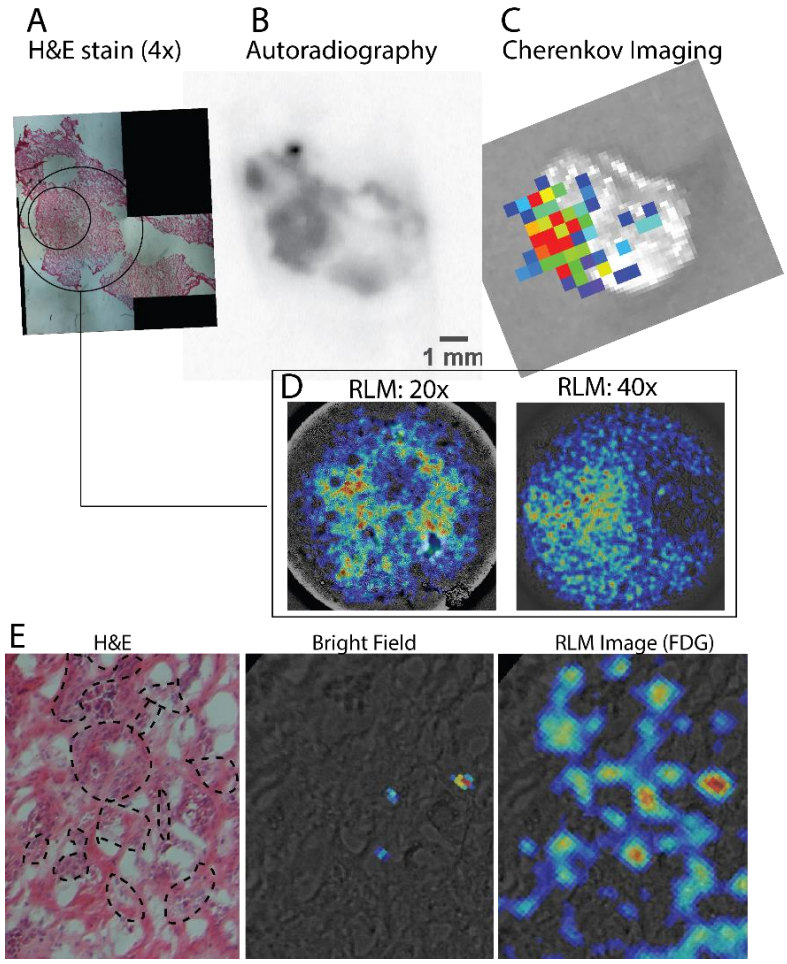

Fig. 5: (A) H&E stain of 10 µm prostate TSC with the field of view of the 20x and 40x RLM image. (B) Autoradiography image of the adjacent prostate TSC with features that are more FDG avid and correlate with cancer in the H&E sample. (C) Cherenkov imaging of the initial prostate TSC (200 µm) reveals a hot spot. (D) RLM image of 10 µm prostate TSC at 20x and 40x magnification. Features can be resolved with a resolution of 80 µm. (E) Correlation of prostate cancer in the TSC with the FDG signal from RLM. Cancerous regions are outlined in the H&E image.

Task 8:

Following the optimization of the protocol (task 8 a & b), we imaged human prostate TSCs, which are shown in Fig. 5. Fig 5 A shows the H&E stain of an entire prostate TSCs following the procedure. These samples are used to determine the Gleason Score. Fig. 5 B shows the autoradiography of an adjacent TSCs slice, where darker regions show higher uptake of radiotracer (FDG). We also used Cherenkov imaging to gauge the localization of the tumor and the ROI for RLM microscopy. The results of the RLM imaging of the FDG distribution in the sample slices is given in Fig 5 D (Task 8 c). This demonstrates that we can continuously image the FDG in prostate TSCs. The structure of the signal easily shows the

improved resolution and thus information contained in these images, when compared to the standard method of autoradiography. Fig. 5 E shows the co-localization of the H&E stain and the FDG distribution in a particular region of interest within the slice (Task 8 d). The method allows for subsequent imaging fixing and H&E staining. RLM allows imaging of the FDG distribution with high resolution and reveals structures with high FDG uptake that have a size of 80 µm, which greatly surpasses the resolution of autoradiography.

Task 9:

We have begun in-vitro imaging of FDG uptake in prostate cancer TSCs and subsequent determination of the local Gleason grades by immunohistochemistry. The results are shown in figure 4. Comparing the FDG signal from suspicious regions to the FDG signal from benign tissue shows a statistically significant difference of 13% ($p=4\times10^{-7}$) when using the mean uptake and a difference of 21% ($p=0.01$) when using the max pixel uptake. By thresholding the FDG signal we can classify the high FDG regions into suspicious tissue. Comparison with H&E information, allows us then to calculate a sensitivity of 0.4 and a specificity of 0.8 for our method. This indicates that FDG does not accumulate in all cancerous regions, but does not give many false positives.

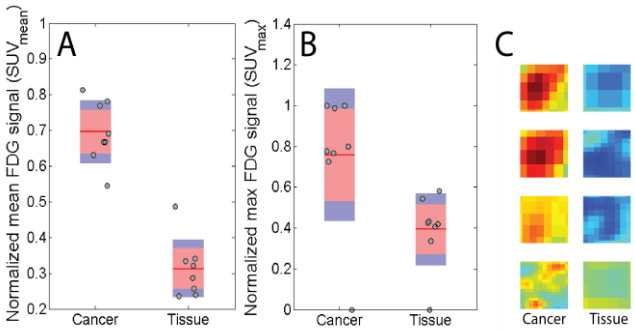

Figure 4: (A) Measured normalized mean FDG signal from RLM of areas determined to be cancer compared to areas designated as healthy. (B) Measured normalized max FDG signal of the same regions. (C) four sample cancer (left) and four tissue (right) regions of interests that were used to determine the values in A&B.

Reportable Outcomes

Objective 1: Design of a radioluminescence microscope for the imaging of FDG uptake in Prostate tissue slice cultures (TSCs).

Research

We successfully completed tasks 1-4 of objective 1. This includes the set-up of an inverted fluorescence microscopy platform to image the FDG distribution in TSCs (task 1). We also developed an algorithm (task 2) that can automatically detect decays and reconstruct the image to give the distribution of radiotracer in the sample. The microscope was calibrated (task 3) and we can determine the local number of radiotracer molecules. The images in figure 3 D show resulting images from FDG in a prostate TSCs in the microscope (task 4).

Training & Mentoring:
The PI received training in handling of radioisotopes and am approved to work with isotopes the Stanford University School of Medicine (Task 5). The PI has completed the course work on Molecular Imaging in Living Subjects (RAD 222), attended and presented at the Molecular Imaging Program at Stanford (MIPS) weekly Seminar series, attended many Radiological Sciences Laboratory (RSL) meetings and presented the RLM microscopy technology at the Annual Biophysical society meeting (task 6).

Objective 2: Comparative measurements of FDG uptake into prostate TSCs of Gleason Grade 3 and 4/5 in vitro.

Research:
We have begun in-vitro imaging of FDG uptake in prostate cancer TSCs and subsequent determination of the local Gleason grades by immunohistochemistry (task 8) and presented initial results in Fig. 4. We have replaced task 7 with a more complex feature detection algorithm, which has led to a project on the endoscopic detection of renal cancer.

These results were presented at the annual World Molecular Imaging Congress in September 2015. The results were not published in a journal article because we will aggregate the results of objective 1 and 2 to publish a more thorough article.

Training & Mentoring:
The PI, Silvan Tuerkcan, is participating in the weekly Peehl laboratory meetings in the Department of Urology and has been exposed to a large overview of prostate cancer topics. The PI has also attended the Cancer Biology course (CBIO 101). The PI has not attended the DoD IMPaCT meeting & Society of Nuclear Medicine Annual Meeting, but he has presented the work at the World Molecular Imaging Congress in September 2015.

The research of aim 2 has trained the PI in Hands-on training in prostate cancer TSCs culturing in bioreactors during the experiments for the optimization of the imaging parameters. The PI was also trained in the determination of the Gleason score by a pathologist.

Conclusion

In summary, the current method is able to measure the uptake of FDG into TSCs from patients, which present a faithful tissue culture model of prostate cancer. The method shows features of down to 80 µm, and shows a significant higher FDG uptake in cancerous regions. Such a set-up can be used to further explore the biology of prostate cancer as well as serve as a base for testing the efficacy of new radiotracers for prostate cancer *in vitro* on patient samples.

We have completed objective 1 and are making progress in objective 2. We have removed task 7 in objective 2, because a change in the design of the experiment delivers better imaging than expected, which removed the requirement for the image correlation algorithm.

References

[1] Warburg O, Wind F, and Negelein E (1927). The Metabolism of Tumors in the Body. J. Gen. Physiol. 8(6), 519-530.
[2] Cairns RA, Harris IS, and Mak TW (2011). Regulation of cancer cell metabolism. Nat. Rev. Canc. 11(2):85-95.
[3] Di Chiro G, De La Paz RL, Brooks RA, Rodney A, Sokoloff L, Kornblith PL et al. (1982). Glucose utilization of cerebral gliomas measured by 18F-fluorodeoxyglucose and positron emission tomography. Neurol. 32(12):1323-1323.
[4] Alavi JB, Alavi A, Chawluk J, Kushner M, Powe J, Hickey W, and Reivich M. (1988). Positron emission tomography in patients with glioma. A predictor of prognosis. Cancer. 62(6):1074–1078.

[5] Pratx G, Chen K, Sun C, Martin L, Carpenter C, Olcott PD, and Xing L. Radioluminescence Microscopy: Measuring the Heterogeneous Uptake of Radiotracers in Single Living Cells. PloS One. 7(10):e46285. 2012.

[6] Pratx G, Chen K, Sun C, Axente M, Sasportas L, Carpenter C, and Xing L, . High-resolution radioluminescence microscopy of FDG uptake by reconstructing the beta ionization track. J. Nucl. Med. 54:1841-1846. 2013.